EEET ECOLOGICAL ENGINEERING & ENVIRONMENTAL TECHNOLOGY

Ecological Engineering & Environmental Technology, 2026, 27(7), 453–470
https://doi.org/10.12912/27197050/224680
ISSN 2719–7050, License CC-BY 4.0

Received: 2026.06.06
Accepted: 2026.06.15
Published: 2026.07.01

Mechanical performance and life-cycle environmental impact of sustainable concrete incorporating rice husk ash and recycled coarse aggregate

Adwan Bahar[1], M. W. Tjaronge[1*], Rita Irmawaty[1]

[1] Department of Civil Engineering, Faculty of Engineering, Universitas Hasanuddin, Gowa 92171, Sulawesi Selatan, Indonesia
* Corresponding author's e-mail: tjaronge@yahoo.co.jp

ABSTRACT

The growing environmental burden of cement manufacturing and natural-aggregate extraction has driven interest in concrete that simultaneously valorises agricultural and construction wastes. This study investigates the mechanical performance and life-cycle environmental impact of sustainable concrete incorporating rice husk ash (RHA) and recycled coarse aggregate (RCA). Three mixtures were evaluated: a control mixture, a mixture with 50% RCA and 20% RHA (50%RCA+20%RHA), and a mixture with 100% RCA and 20% RHA (100%RCA+20%RHA). The compressive strength, axial stress–strain behaviour, peak stress and strain, static modulus of elasticity, and toughness were determined and compared with the Popovics and Carreira and Chu constitutive models, while the environmental performance was quantified through a cradle-to-gate life-cycle assessment (LCA) covering embodied energy (EE), global warming potential (GWP), acidification potential (AP), eutrophication potential (EP), and photochemical ozone creation potential (POCP), each normalised by compressive strength and analysed using multi-criteria decision-making (MCDM). The compressive strength decreased from 27.35 MPa for the control to 25.93 and 22.55 MPa at 50% and 100% RCA, and the modulus of elasticity fell more sharply than the strength, while moderate (50%) RCA combined with 20% RHA produced the highest toughness and toughness index. Because the Popovics and Carreira & Chu models share the same three-parameter formulation, fitting the peak-strain and shape parameters to each curve makes the two models coincide; the resulting unified model reproduced the measured stress–strain response of all three mixtures with a coefficient of determination $R^2 \geq 0.993$ and a root-mean-square error of 0.23–0.78 MPa. The 100%RCA+20%RHA mixture achieved the largest reductions in EE, GWP, AP, EP, and POCP (about 18.3%, 18.5%, 30.7%, 6.8%, and 85.1%, respectively) relative to the control, whereas the 50%RCA+20%RHA mixture offered the most balanced impact-to-strength ratios. The MCDM analysis ranked the 100%RCA+20%RHA mixture highest under the adopted weighting scenario, confirming that the combined use of RHA and RCA can deliver structurally viable, markedly lower-impact concrete when the RCA replacement level is appropriately selected. As the assessment is limited to 28-day mechanical and cradle-to-gate environmental performance, durability and cost validation remain necessary before structural deployment.

Keywords: rice husk ash, recycled coarse aggregate, stress–strain behaviour, modulus of elasticity, toughness, life-cycle assessment.

INTRODUCTION

Concrete is the most widely used construction material worldwide, with production exceeding tens of billions of tonnes annually. However, its extensive use is associated with significant environmental impacts. Ordinary Portland cement (OPC) production alone accounts for approximately 8–10% of global anthropogenic carbon dioxide emissions due to limestone calcination and the combustion of fossil fuels during clinker manufacturing (Suomie et al., 2025). At the same time, continuous extraction of natural aggregates depletes non-renewable resources, while the construction and demolition (C&D) sector generates enormous quantities of waste.

Recent estimates indicate that more than 3 billion tonnes of C&D waste are produced annually worldwide, with China contributing over 2 billion tonnes, the United States approximately 600 million tonnes, and the European Union around 850 million tonnes (Patil, 2024; Eurostat, 2022). In Indonesia, rapid urbanization and infrastructure development have increased demolition waste generation, leading the government to classify C&D waste as "specific waste" under Government Regulation No. 27 of 2020. Nevertheless, recycling rates remain limited, and most waste is still disposed of in landfills or open dumping sites (Government Regulation No. 27/2020). These challenges have stimulated research into sustainable concrete systems capable of reducing raw-material consumption and environmental impacts while maintaining adequate structural performance.

One promising approach is the replacement of natural coarse aggregate (NCA) with recycled coarse aggregate (RCA) derived from crushed C&D waste. The use of RCA diverts waste from landfills and reduces dependence on virgin aggregate resources (Suomie et al., 2025). However, RCA differs from NCA because it contains adhered mortar from the original concrete. This residual mortar is porous and micro-cracked, resulting in higher water absorption, lower density, and inferior mechanical properties compared with natural aggregates. Consequently, RCA generally reduces workability and may negatively affect hardened concrete performance (Ahmad et al., 2023).

The presence of adhered mortar also creates an additional and weaker interfacial transition zone (ITZ) between the old mortar and the new cement paste. These weak ITZs facilitate crack initiation and propagation, leading to reductions in compressive strength and modulus of elasticity while increasing peak strain and post-peak brittleness. Previous studies have shown that moderate RCA replacement levels of up to approximately 50% can still satisfy structural requirements, whereas higher replacement levels tend to cause more significant losses in strength and stiffness, with reductions in elastic modulus often exceeding those in compressive strength (Shah et al., 2021; Plaza et al., 2021; Suomie et al., 2025).

In addition to aggregate recycling, replacing a portion of cement with supplementary cementitious materials (SCMs) is an effective strategy for reducing the environmental footprint of concrete. Rice husk ash (RHA), an agricultural by-product generated from rice husk combustion, is particularly attractive in rice-producing countries such as Indonesia (Suomie et al., 2025). Global rice production generates millions of tonnes of RHA annually, while Indonesia alone produces approximately 54 million tonnes of paddy each year (BPS-Statistics Indonesia, 2024). Much of this biomass waste remains underutilized despite its considerable potential as a cement substitute.

When produced under controlled combustion conditions and finely ground, RHA contains a high proportion of amorphous silica, which exhibits strong pozzolanic reactivity. This silica reacts with calcium hydroxide released during cement hydration, forming additional calcium silicate hydrate (C–S–H) gel that refines the pore structure and strengthens the ITZ. As a result, RHA incorporation generally improves mechanical and durability properties up to an optimum replacement level of approximately 10–20%, beyond which dilution effects may reduce strength (Suomie et al., 2025).

The combination of RCA and RHA is particularly attractive because both materials address complementary sustainability challenges. RCA promotes the recycling of construction waste and reduces natural aggregate consumption, while RHA utilizes agricultural waste and lowers cement demand. Furthermore, the pozzolanic reaction of RHA can improve the quality of the ITZ surrounding RCA particles, partially compensating for the weaknesses associated with adhered mortar. Consequently, the combined use of RCA and RHA has the potential to produce concrete with improved sustainability and acceptable structural performance (Suomie et al., 2025). Recent studies have confirmed that reactive SCMs can recover a significant portion of the mechanical performance lost due to RCA incorporation while simultaneously reducing environmental impacts (Ma et al., 2024).

Despite these advantages, research on concrete containing both RHA and RCA remains limited. Most existing studies focus primarily on compressive strength, while comparatively little attention has been paid to the complete stress–strain response, modulus of elasticity, and toughness characteristics that are important for structural applications. According to the recent review by Suomie et al. (2025), the combined use of RHA and RCA is still underexplored, and many investigations evaluate these materials separately

rather than examining their synergistic effects. In addition, the applicability of established constitutive models such as those proposed by Popovics (1973) and Carreira and Chu (1985) has not been extensively verified for concrete containing both RHA and high levels of RCA. Environmental assessments are also often conducted independently from mechanical evaluations, despite sustainability being the primary motivation for incorporating these materials.

Despite the growing number of studies on RCA and RHA, previous investigations have primarily focused on either mechanical performance, durability behaviour, or environmental assessment as separate research topics. In addition, the applicability of existing constitutive stress–strain models to concrete incorporating both RCA and RHA has received limited attention, while the integration of mechanical performance, constitutive modelling, life-cycle environmental assessment, and multi-criteria sustainability evaluation within a single experimental framework remains scarce.

Accordingly, this study provides a comprehensive assessment of concrete containing 20% RHA and up to 100% RCA by combining experimental mechanical characterization, evaluation of existing constitutive stress–strain models, cradle-to-gate life-cycle assessment, and multi-criteria sustainability analysis. Through this integrated approach, the study seeks to evaluate the potential of agricultural and construction-demolition waste valorization through the simultaneous assessment of structural performance and environmental impacts. It is expected that the findings will contribute to the development of a decision-support framework for selecting sustainable concrete mixtures that balance engineering performance with environmental benefits within a circular-economy context.

EXPERIMENTAL PROCEDURE

Materials

PCC conforming to the relevant national standard was used as the primary binder. River sand was used as the natural fine aggregate, and crushed stone was used as the natural coarse aggregate (NCA), both satisfying the grading requirements of ASTM C33. The RCA was produced by crushing laboratory waste concrete and was used to replace the natural coarse aggregate on a mass basis at the prescribed substitution levels. RHA, obtained from the controlled combustion of rice husks and ground to a fineness suitable for pozzolanic use, was employed as a partial replacement for cement. A polycarboxylate-based superplasticizer (Sika ViscoCrete) was added to maintain adequate workability at the low effective water content, and clean potable water was used for both mixing and curing. To compensate for its high-water absorption and to prevent it from withdrawing water from the fresh paste, the RCA was conditioned to a saturated surface-dry (SSD) state prior to batching. The constituent materials used in this study are shown in Figure 1.

The physical characteristics of the constituent materials are summarized in Table 1. The recycled coarse aggregate exhibited a substantially higher water absorption (13.02%) than the natural coarse aggregate (1.53%), together with a slightly lower bulk specific gravity (2.41 versus 2.58 on an SSD basis), reflecting the porous adhered mortar that characterizes RCA. The fineness modulus of the recycled and natural coarse aggregates was comparable (7.49 and 7.44, respectively), confirming that the RCA was processed to a grading similar to that of the NCA. The particle-size distributions of the fine aggregate, NCA, and RCA are presented in Figure 2; all three gradings fall within the corresponding ASTM C33 upper and lower limits.

The chemical composition and physical properties of the PCC and RHA are presented in Table 2. The cement was dominated by calcium oxide (CaO, 58.45%), consistent with its primary role in the formation of calcium silicate hydrate during hydration. The RHA was composed mainly of silica (SiO_2, 51.12%) together with a substantial proportion of iron oxide (Fe_2O_3, 29.26%), the silica providing the reactive phase responsible for its pozzolanic behaviour. The contents of other oxides, including MgO (0.67%), K_2O (0.16%), TiO_2 (0.09%), MnO (0.79%), and SO_3 (0.76%), were comparatively lower. The specific gravity of the RHA (2.08) was appreciably lower than that of the PCC (3.20), reflecting the porous, lightweight nature of the ash.

Mix proportions and specimen preparation

Three concrete mixtures were designed in this study: a control mixture without recycled materials (control), a mixture containing 50% RCA as a coarse-aggregate

Figure 1. Constituent materials used in this study

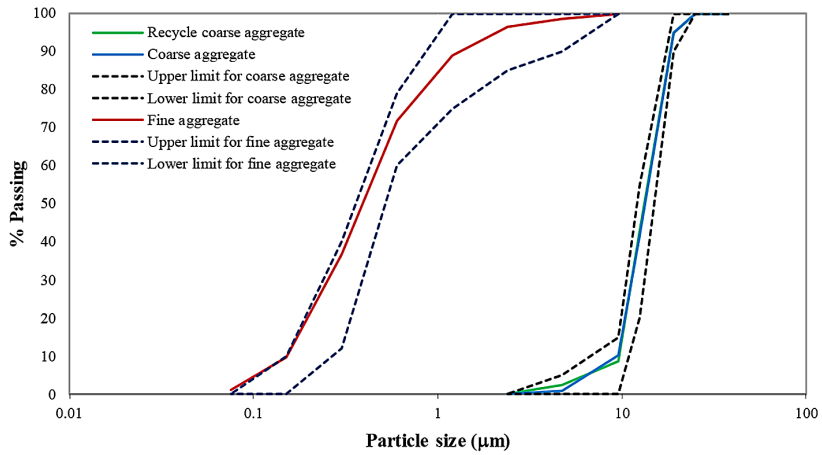

Figure 2. Particle-size distribution of the fine aggregate, natural coarse aggregate, and recycled coarse aggregate relative to the ASTM C33 grading limits

Table 1. Physical characteristics of constituent materials

Material	Apparent specific gravity	Bulk specific gravity (OD basis)	Bulk specific gravity (SSD basis)	Fineness modulus	Moisture content (%)	Water absorption (%)
RCA	2.91	2.14	2.41	7.49	5.79	13.02
Coarse aggregate (NCA)	2.67	2.55	2.58	7.44	1.82	1.53
Fine aggregate	2.54	2.37	2.44	1.99	2.21	2.81

replacement together with 20% RHA as a cement replacement (50%RCA+20%RHA), and a mixture containing 100% RCA with 20% RHA (100%RCA+20%RHA). In all mixtures the RHA replacement was fixed at 20% by mass of cement, while the RCA replacement level was varied so that its effect on mechanical and environmental performance could be isolated. The detailed mix proportions of the constituent materials are summarized in Table 3.

For each mixture, three cylindrical specimens (n = 3) measuring Ø100 × 200 mm were cast for compressive-strength evaluation. The fresh concrete was placed into the cylindrical moulds and compacted to ensure adequate consolidation. The specimens were kept under ambient

Table 2. Chemical composition and physical properties of PCC and RHA

Material property	CaO	SiO_2	Al_2O_3	Fe_2O_3	SO_3	MgO	K_2O	TiO_2	MnO	LOI	Others	Specific gravity
PCC	58.45	13.41	3.47	3.52	2.29	0	0.4	0.25	0.21	17.89	0.11	3.2
RHA	1.57	51.12	2.84	29.26	0.76	0.67	0.16	0.09	0.79	10.43	2.31	2.08

Table 3. Mix proportions of the concrete mixtures by weight per m^3

Mix ID	Water	PCC	Fine Agg.	NCA	RCA	RHA	ViscoCrete
Control	197	469.34	652.63	1003.28	0.00	0.00	3.06
50%RCA+20%RHA	197	375.46	652.63	501.63	468.58	61.01	3.06
100%RCA+20%RHA	197	375.46	652.63	0.00	937.18	61.01	3.06

laboratory conditions for 24 h before demoulding, after which they were immersed in water and cured for 28 days prior to testing.

Compressive strength

The compressive-strength test was carried out in accordance with ASTM C39 using a universal testing machine (UTM) with a maximum loading capacity of 2000 kN (Figure 3). The axial load was applied to the end surface of each cylinder at a constant rate of 0.2 MPa/s until failure. The compressive strength was determined by divide maximum load to its surface area of specimens.

Axial stress–strain behaviour and constitutive modelling

During the compression test, the applied load and the corresponding axial deformation were recorded continuously to construct the complete axial stress–strain curve of each mixture, capturing both the ascending and the descending branches. The axial stress at each instant was obtained by dividing the load by the specimen cross-sectional area, and the axial strain was obtained from the measured axial deformation over the gauge length. The experimental curves were then compared with two widely used uniaxial constitutive models for concrete in compression, the Popovics (1973) model and the Carreira & Chu (1985) model to assess their applicability to RHA–RCA concrete. The two models describe the normalised stress–strain relationship in the forms given by Equations 1 and 2. Both expressions reduce to the same three-parameter function of the peak stress f′c, the peak (reference) strain ε₀, and a curve-shape parameter. For each mixture, f′c was fixed at the measured peak stress, while ε₀ and shape parameter were obtained by least-squares regression of the model to the complete experimental curve using the Levenberg–Marquardt algorithm. The quality of the fit was then quantified by the coefficient of determination (R^2), the root-mean-square error (RMSE), and the mean absolute error (MAE) computed between the measured and predicted stresses at the experimental strain points.

$$\sigma = f'c \cdot n(\varepsilon/\varepsilon_0) / [\, n - 1 + (\varepsilon/\varepsilon_0)^n \,] \quad (1)$$

$$\sigma = f'c \cdot \beta(\varepsilon/\varepsilon_0) / [\, \beta - 1 + (\varepsilon/\varepsilon_0)^\beta \,] \quad (2)$$

Figure 3. Compressive-strength test setup on the universal testing machine (UTM)

The dimensionless shape parameter (n for the Popovics model and β for the Carreira & Chu model) can be estimated from the secant relationship between strength, peak strain, and modulus of elasticity, as expressed in Equation 4 and 5.

$$n = 1 + 0.058\, f'c \tag{3}$$

$$\beta = 1 / [\, 1 - f'c / (\varepsilon_0 \cdot Ec)\,] \tag{4}$$

where: σ is the axial stress, $f'c$ is the peak (compressive) stress, ε is the axial strain, ε_0 is the strain corresponding to the peak stress, Ec is the modulus of elasticity, and n and β are dimensionless parameters that control the shape of the curve, particularly the steepness of the post-peak descending branch. The peak-stress strain ε_0 and the shape parameters were determined from the experimental curves and used to evaluate how closely each model reproduced the measured behaviour of the control and recycled mixtures.

Modulus of elasticity

The static modulus of elasticity of each mixture was determined from the initial, approximately linear portion of the ascending branch of the axial stress–strain curve, following the chord-modulus concept defined in ASTM C469. For comparison, the modulus was also extracted from the fitted Popovics and Carreira & Chu curves, allowing the model predictions to be evaluated directly against the experimental values.

Toughness and toughness index

Toughness, taken as a measure of the energy-absorption capacity of the concrete, was evaluated as the area enclosed under the axial stress–strain curve, as expressed in Equation 5.

$$T = \int \sigma \, d\varepsilon \tag{5}$$

The toughness index (TI) was defined as the ratio of the energy absorbed up to a specified post-peak strain to the energy absorbed up to the peak-stress strain, as given in Equation 6.

$$TI = T_{post\text{-}peak} / T_{peak} \tag{6}$$

A higher toughness index indicates greater post-peak ductility and a more gradual loss of load-carrying capacity beyond the peak. Both the toughness and the toughness index were computed from the experimental curves and from the Popovics and Carreira & Chu model predictions in order to evaluate the influence of the RCA replacement level on the energy-absorption behaviour of the RHA–RCA mixtures.

Life cycle assessment (environmental impact)

The environmental performance of each mixture was evaluated using a life-cycle assessment (LCA) approach at the cradle-to-gate stage, which includes the impacts associated with raw material extraction, processing, manufacturing, and transportation of constituent materials (Guinée et al., 2002). Five impact categories were assessed, namely embodied energy (EE), global warming potential (GWP), acidification potential (AP), eutrophication potential (EP), and photochemical ozone creation potential (POCP).

Embodied energy represents the total energy consumed throughout the material life cycle, including extraction, processing, manufacturing, transportation, and construction activities (Dixit et al., 2010). In concrete production, EE is strongly governed by Portland cement consumption because clinker manufacturing requires high-temperature calcination and intensive fossil fuel combustion (Flower and Sanjayan, 2007). Consequently, cement production contributes significantly to the overall environmental burden and carbon emissions of concrete (Cabeza et al., 2014; Habert et al., 2011).

Global warming potential reflects greenhouse gas emissions, particularly CO_2, CH_4, and N_2O, expressed in kg CO_2-equivalent (Stocker et al., 2014). Acidification potential is associated with emissions such as SO_2, NO_x, and NH_3 that contribute to acid rain and ecosystem degradation. Eutrophication potential describes the enrichment of water bodies caused by excessive nutrient emissions from industrial and extraction activities (Bare et al., 2002). Meanwhile, POCP refers to ground-level ozone formation resulting from photochemical reactions between VOCs and NO_x under sunlight exposure (An et al., 2024). In concrete manufacturing, these impacts mainly originate from cement production, transportation, electricity consumption, and aggregate processing (Flower and Sanjayan, 2007).

Because cement production is highly energy-intensive, the incorporation of supplementary cementitious materials (SCMs) has been widely recognized as an effective strategy to reduce EE,

GWP, AP, EP, and POCP while maintaining satisfactory mechanical performance (Habert et al., 2011). The reference impact factors for water, PCC, fine aggregate, coarse aggregate, RCA, RHA, and ViscoCrete superplasticizer were adopted from published studies and environmental product declarations, as summarized in Table 4.

For each mixture, the total value of a given impact category was obtained by summing the products of the reference impact factor and the corresponding mass of each constituent, as expressed in Equation 7.

$$E = \Sigma (N_i \cdot W_i) \quad (7)$$

where: E is the environmental impact for a given category (EE, GWP, AP, EP, or POCP), Ni is the reference impact factor of constituent-i for that category, and Wi is the mass of constituent i in the mixture (kg/m³). To evaluate environmental efficiency relative to structural performance, each impact value was normalized by the average 28-day compressive strength of the mixture to obtain the environmental impact-to-strength ratio, as defined in Equation 8.

$$\textit{Environmental impact-to-strength ratio} = E / f'c \quad (8)$$

The resulting EE/f'c, GWP/f'c, AP/f'c, EP/f'c, and POCP/f'c ratios provide a consistent basis for comparing the mixtures while accounting for differences in compressive strength. Finally, the overall environmental–mechanical performance of the mixtures was ranked using the Technique for Order of Preference by Similarity to the Ideal Solution (TOPSIS), one of the most widely applied multi-criteria decision-making (MCDM) methods for sustainable-concrete mix selection (Hwang and Yoon, 1981; Rashid et al., 2020). The five impact-to-strength ratios were arranged in a decision matrix and treated as non-beneficial (cost) criteria, since lower values denote better environmental efficiency. Each criterion was vector-normalised by dividing every entry by the square root of the sum of squares of its column, and equal weights (w = 0.20) were assigned in the absence of a stakeholder-derived weighting. The positive ideal solution was taken as the minimum and the negative ideal solution as the maximum of each weighted normalised criterion. The Euclidean separation of each mixture from the two ideal solutions, d^+ and d^-, was computed, and the relative closeness coefficient $C_h = d^- / (d^+ + d^-)$ was used as the ranking score, where a higher C_h denotes a more favourable overall performance. A radar chart of the same normalised indicators is retained solely as a visualisation, not as the ranking criterion, and a one-criterion-at-a-time sensitivity check was performed to identify which indicator governs the ranking.

RESULTS AND DISCUSSION

Compressive strength

Figure 4 illustrates the 28-day compressive strength of the concrete mixtures containing rice husk ash (RHA) and recycled concrete aggregate (RCA). The control mixture exhibited the highest compressive strength, reaching approximately

Table 4. Environmental impact parameters for each concrete constituent

Material	EE (MJ)	GWP (kg CO_2 eq)	AP (kg SO_2 eq)	EP (kg PO_4 eq)	POCP (kg C_2H_4 eq)
Water	1.00E-02 (Kina and Turk, 2025)	1.89E-04 (Shi, 2021)	5.16E-03 (Huang, 2025)	6.57E-05 (Kim, 2016)	4.86E-07 (Kim, 2016)
PCC	4.73E+00 (Kina and Turk, 2025)	9.48E-01 (Kim, 2016)	1.62E+00 (Huang, 2025)	1.34E-04 (Kim, 2016)	2.43E-03 (Kim, 2016)
Fine aggregate	3.70E-02 (Kumar et al., 2021)	9.87E-03 (Ohemeng and Naghizadeh, 2023)	1.01E-02 (Huang, 2025)	1.92E-03 (Kim, 2016)	1.07E-04 (Kim, 2016)
Coarse aggregate	4.00E-01 (Cherian et al., 2020)	1.43E-02 (Park et al., 2019)	1.63E-01 (Huang, 2025)	7.27E-06 (EPD MD-25171-EN, 2025)	2.52E-02 (EPD MD-25171-EN, 2025)
RCA	3.00E-01 (Hammond and Jones, 2011)	2.94E-02 (Park et al., 2019)	3.02E-02 (Huang, 2025)	5.44E-06 (Park, 2019)	1.25E-05 (Park et al, 2019)
RHA	2.20E-02 (Tejeswara et al., 2026)	2.70E-03 (Fernando et al., 2021)	2.22E-01 (Ro et al., 2024)	2.50E-05 (Zhao et al., 2024)	4.10E-02 (Zhao et al., 2024)
ViscoCrete	3.68E+01 (Hammond and Jones, 2011)	7.39E-01 (Saade et al., 2020)	2.92E-03 (Mohammad et al., 2025)	1.03E-03 (Mohammad et al., 2025)	2.12E-04 (Mohammad et al., 2025)

27.35 MPa, followed by the mixture incorporating 50%RCA+20%RHA with a compressive strength of around 25.93 MPa. Meanwhile, the 100%RCA+20%RHA mixture showed the lowest strength value, approximately 22.55 MPa. The results indicate that the partial replacement of natural aggregate with RCA led to a gradual reduction in compressive strength, particularly at higher RCA substitution levels. Nevertheless, the mixture containing 50% RCA still demonstrated a relatively comparable strength to the control mixture, suggesting that moderate RCA incorporation can maintain acceptable mechanical performance. The error bars also reveal relatively small variability among specimens, indicating good consistency in the experimental results.

The reduction in compressive strength observed in mixtures with higher RCA content can be attributed to the weaker interfacial transition zone (ITZ) and the presence of adhered old concrete attached to recycled aggregates. RCA generally possesses higher porosity and water absorption compared to natural aggregates, which may increase internal microcracking and reduce the overall density of the concrete matrix. In addition, although RHA contributes to pozzolanic reactions through the formation of additional calcium silicate hydrate (C–S–H) gel, its beneficial effect appears insufficient to fully compensate for the mechanical deficiencies introduced by the complete replacement of natural aggregates with RCA. Consequently, the 100%RCA+20%RHA mixture exhibited the most pronounced strength reduction. These findings suggest that the combined utilization of RHA and RCA can still produce structurally viable concrete when the RCA replacement ratio is properly controlled, thereby supporting the development of more sustainable concrete materials with reduced environmental impact.

Stress-strain curve

The axial compressive stress–strain behaviour was measured for the control, 50%RCA+20%RHA, and 100%RCA+20%RHA mixtures, and the curves of the individual specimens together with their averages are presented in Figures 5(a)–(c). For all mixtures the response began with an approximately linear ascending branch up to about 40–50% of the peak stress, followed by a gradually flattening curve until the peak was reached, and then a descending (softening) branch. As the RCA replacement level increased, the peak stress decreased and the descending branch became progressively steeper, indicating a more rapid loss of load-carrying capacity beyond the peak. This behaviour is characteristic of recycled aggregate concrete and is associated with the weaker, more porous interfacial transition zone (ITZ) introduced by the adhered mortar of the RCA, which promotes earlier micro-crack coalescence under load (Liu et al., 2022; Ma et al., 2024).

An analytical model based on the stress–strain relationships proposed by Popovics and Carreira–Chu was developed for RCA–RHA concrete. Since the Popovics and Carreira–Chu models are algebraically identical, differing only in the notation of the dimensionless shape parameter (n in the Popovics model and β in the Carreira–Chu model), both can be represented by the unified three-parameter relationship given in Equation 9:

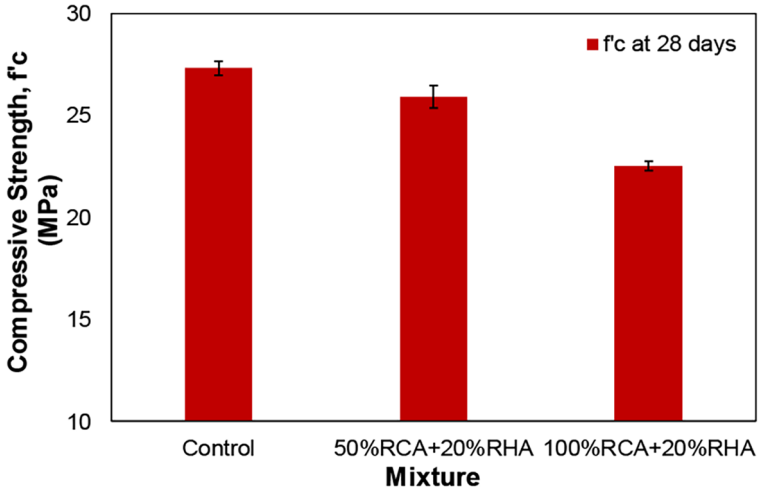

Figure 4. Compressive strength of concrete mixtures

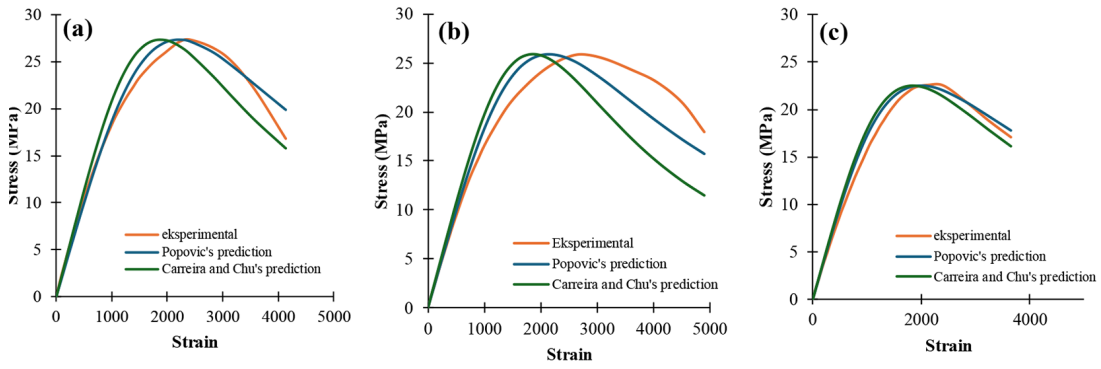

Figure 5. Stress-strain relationship of: (a) control, (b) 50%RCA+20%RHA, and (c) 100%RCA+20%RHA specimens

$$\sigma = (f'c \times k \times (\varepsilon/\varepsilon_0)) / (k - 1 + (\varepsilon/\varepsilon_0)^k) \quad (9)$$

where: σ is the axial stress, ε is the axial strain, $f'c$ is the measured peak compressive stress, ε_0 is the strain at peak stress, and k ($\equiv$ n $\equiv$ β) is a dimensionless parameter governing the curvature of the ascending and descending branches of the stress–strain curve.

In this study, ε_0 and k were obtained for each mixture through least-squares regression of the unified model to the complete experimental stress–strain data, while $f'c$ was fixed at the measured peak stress. The fitted parameters and corresponding goodness-of-fit values are presented in Figure 6 and Table 5.

The fitted model reproduced the complete ascending and descending response of every mixture (Figure 6), with R^2 = 0.993, 0.997 and 0.999 and RMSE = 0.78, 0.51 and 0.23 MPa for the control, 50%RCA+20%RHA and 100%RCA+20%RHA mixtures, respectively (Table 5). The corresponding fitted parameters were ε_0 = 2184, 2539 and 2095 με and k = 2.761, 2.292 and 2.672, with the fitted ε_0 falling within 91–99% of the measured peak strain because the experimental peak is comparatively flat. These results confirm that the established uniaxial formulation remains applicable to combined RHA–RCA concrete without developing a new model, and that neither classical model is intrinsically superior once their common parameters are fitted to the data (Ma et al., 2024).

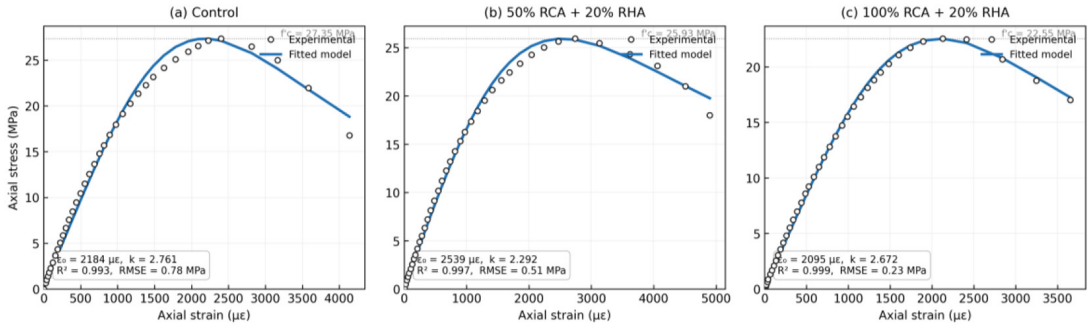

Figure 6. Experimental versus fitted unified uniaxial constitutive model for (a) control, (b) 50%RCA+20%RHA, and (c) 100%RCA+20%RHA mixtures (f'c fixed at the measured peak; ε_0 and k regression-fitted)

Table 5. Fitted unified uniaxial constitutive model: parameters (f'c fixed at measured peak; ε_0 and k regression-fitted) and goodness of fit for each mixture

Mixture	f'c (MPa)	ε_0 (με)	k	R^2	RMSE (MPa)	MAE (MPa)
Control	27.35	2184	2.761	0.993	0.78	0.65
50%RCA+20%RHA	25.93	2539	2.292	0.997	0.51	0.38
100%RCA+20%RHA	22.55	2095	2.672	0.999	0.23	0.19

Peak stress

The experimental and model-predicted peak (compressive) stresses of the three mixtures are compared in Figure 7 and summarized in Table 6. The control mixture developed the highest peak stress (27.35 MPa), followed by the 50%RCA+20%RHA mixture (25.93 MPa) and the 100%RCA+20%RHA mixture (22.55 MPa), corresponding to reductions of approximately 5.2% and 17.6% relative to the control.

The progressive decrease with increasing RCA content is consistent with the lower strength and higher porosity of the recycled aggregate and the weaker ITZ, which cannot be fully offset by the pozzolanic contribution of the 20% RHA (Shah et al., 2021; Suomie et al., 2025). Both constitutive models predicted the peak stress almost exactly, with the Popovics values (27.35, 25.89 and 22.51 MPa) and the Carreira & Chu values (27.31, 25.93 and 22.54 MPa) deviating from the measured results by less than 0.2%, since the peak stress is an input anchor common to both models.

Peak strain

Figure 8 presents the axial strain at peak stress (ε_0, in microstrain) for the three mixtures together with the model predictions. The measured peak strain increased from 2400.59 με for the control to 2737.65 με for the 50%RCA+20%RHA mixture, before decreasing to 2126.13 με for the 100%RCA+20%RHA mixture. The higher peak strain of the 50% RCA mixture reflects the greater deformability imparted by the more compliant recycled aggregate and its porous adhered mortar, whereas the lower value at full replacement is associated with the markedly reduced strength and the more brittle, micro-crack-dominated response of the 100% RCA matrix (Ma et al., 2024). The Popovics model predicted peak strains of 2228.22, 2241.77 and 1894.49 με, and the Carreira & Chu model predicted 1955.87, 1853.90 and 1894.49 με; both models tended to underestimate the measured peak strain, the deviation being largest for the 50% RCA mixture, which indicates that the strain capacity of the recycled mixtures is slightly greater than that implied by the empirical strain expressions calibrated on natural aggregate concrete.

Modulus of elasticity

The static modulus of elasticity of the three mixtures, determined from the initial linear portion of the stress–strain curve, is compared with the model predictions in Figure 9 and Table 6. The experimental modulus decreased steadily with increasing RCA content, from 20473.90 MPa for the control to 18408.26 MPa (−10.1%) for the 50%RCA+20%RHA mixture and 17211.62 MPa (−15.9%) for the 100%RCA+20%RHA mixture. The reduction in stiffness exceeded the corresponding reduction in peak stress, confirming the well-established observation that RCA lowers the elastic modulus more severely than the compressive strength, owing to the low stiffness and high porosity of the adhered mortar (Plaza et al., 2021; Suomie et al., 2025). In contrast to the experimental trend, both models predicted only a mild decrease in modulus with RCA content, Popovics giving 19841.18, 19687.41 and 19401.64 MPa and Carreira & Chu giving 22623.44, 21400.22 and 20270.46 MPa because the modulus in these formulations is governed primarily by the compressive strength and

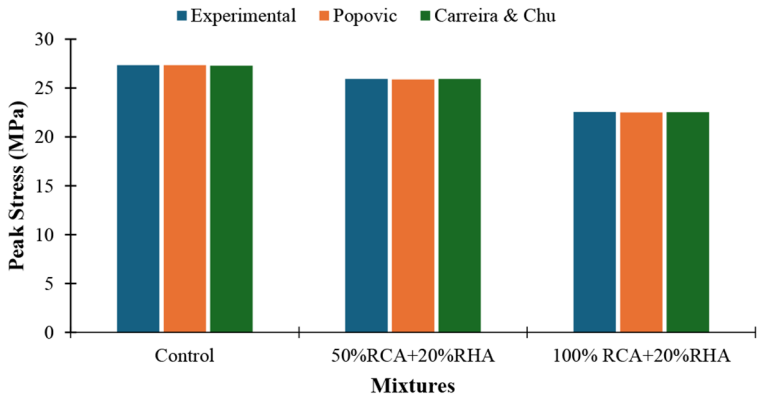

Figure 7. Peak stress of control, 50%RCA+20%RHA, and 100%RCA+20%RHA mixtures with existing constitutive models

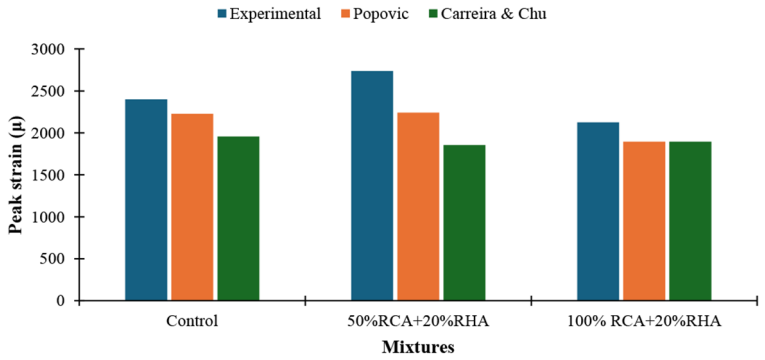

Figure 8. Peak strain of control, 50%RCA+20%RHA, 100%RCA+20%RHA with existing constitutive models

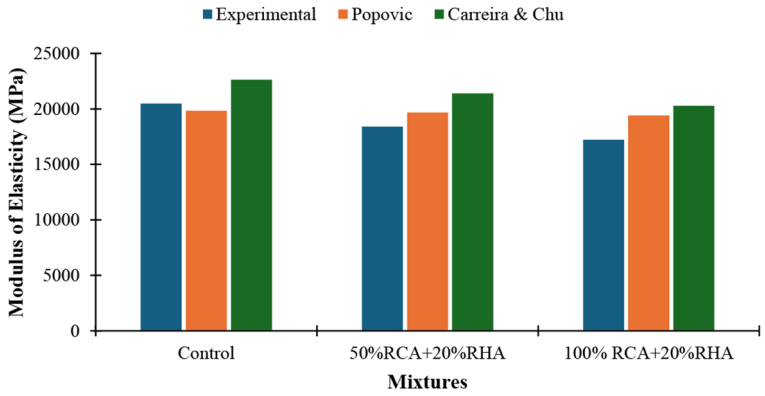

Figure 9. Modulus of elasticity of control, 50%RCA+20%RHA, 100%RCA+20%RHA with existing constitutive models

assumed density. As a result, the models slightly underestimated the stiffness of the control mixture but increasingly overestimated that of the high-RCA mixtures, the largest discrepancy occurring for the 100%RCA+20%RHA mixture.

Toughness and toughness index

The toughness, taken as the area under the axial stress–strain curve, and the toughness index of the three mixtures are summarized in Table 7. The experimental toughness was 73.995 kJ/m³ for the control, increased slightly to 77.556 kJ/m³ for the 50%RCA+20%RHA mixture, and then decreased to 63.381 kJ/m³ for the 100%RCA+20%RHA mixture. The improvement at 50% RCA reflects the greater energy absorbed during the more gradual, ductile softening of that mixture, whereas the reduction at full replacement follows from its substantially lower peak stress. The experimental toughness index showed the same ranking, rising from 1.69 for the control to 1.94 for the 50%RCA+20%RHA mixture and then easing to 1.80 for the 100%RCA+20%RHA mixture,

Table 6. Comparison of experimental results and predictions from the Popovics and Carreira–Chu models for RHA–RCA concrete

Mixtures	Experimental f'c (MPa)	Peak Strain		Modulus of elasticity (MPa)		β		ε_0	
		Popovics	Carreira & Chu	Popovics	Carreira & Chu	Popovics	Carreira & Chu	Popovics	Carreira & Chu
Control	27.35	0.93	0.81	0.97	1.10	2.59	2.74	2204.98	1874.19
50%RCA +20%RHA	25.93	0.82	0.68	1.07	1.16	2.50	2.78	2145.77	1864.10
100%RCA +20%RHA	22.55	0.89	0.89	1.13	1.18	2.31	2.44	1991.39	1840.11

Table 7. Experimental and predicted toughness and toughness index of the RHA–RCA concrete mixtures based on the Popovics and Carreira & Chu models

Mixtures	Toughness (kJ/m³)			Toughness Index		
	Experimental	Popovic	Carreira & Chu	Experimental	Popovic	Carreira & Chu
Control	73.995	99.694	77.556	1.69	2.05	1.94
50%RCA+20%RHA	77.556	73.405	63.238	1.94	1.88	2.27
100%RCA+20%RHA	63.381	59.041	55.774	1.80	1.92	1.95

indicating that moderate RCA replacement combined with 20% RHA yields the most favourable post-peak ductility. This enhanced energy-absorption capacity is consistent with reports that pozzolanic RHA promotes a more ductile, energy-dissipating fracture pattern through progressive micro-cracking rather than abrupt failure (Ma et al., 2024). The Popovics and Carreira & Chu models reproduced the experimental ranking reasonably well: the Popovics toughness indices (2.05, 1.88 and 1.92) and the Carreira & Chu indices (1.94, 2.27 and 1.95) bracket the measured values; because the two models share the same functional form, they coincide once their parameters are fitted to each curve, so neither yields a systematically closer estimate of the energy-absorption behaviour.

Life-cycle assessment (environmental impact)

Figure 10 presents the LCA results of the concrete mixtures, including both the absolute environmental impact indicators and the corresponding impact-to-strength ratios. The environmental indicators quantify the total environmental burden associated with concrete production, whereas the impact-to-strength ratios provide a measure of environmental efficiency by relating each impact category to the compressive strength achieved by the mixtures.

Embodied energy and energy-to-strength ratio

Figure 10(a) shows that incorporating 20% RHA and RCA significantly reduced embodied energy (EE). The control mixture recorded the highest EE (968.140 MJ/m³), while the 50%RCA+20%RHA and 100%RCA+20%RHA mixtures achieved values of 810.595 and 791.152 MJ/m³, representing reductions of 16.3% and 18.3%, respectively. This improvement is attributed to the lower energy demand of RCA processing and the partial replacement of PCC with RHA, which reduced clinker consumption (Hammond and Jones, 2011).

A similar trend was observed for the EE/f'c ratio. The 50%RCA+20%RHA mixture exhibited the lowest EE/f'c value (31.265 MJ/MPa), compared with 35.398 MJ/MPa for the control, indicating the most efficient balance between energy demand and compressive strength. Although the 100%RCA+20%RHA mixture achieved the lowest EE, its EE/f'c value (35.084 MJ/MPa) was comparable to the control due to the greater reduction in compressive strength. Therefore, moderate RCA replacement provided the most favorable energy-to-strength performance.

Global warming potential and GWP-to-strength ratio

Figure 10(b) shows that incorporating RHA and RCA significantly reduced the global warming potential (GWP) of concrete. The control mixture exhibited the highest GWP (149.429 kg CO_2/m³), while the 50%RCA+20%RHA and 100%RCA+20%RHA mixtures achieved values of 124.636 and 127.572 kg CO_2/m³, corresponding to reductions of 16.6% and 14.6%, respectively. This reduction is primarily attributed to the lower PCC content resulting from RHA substitution, which decreased clinker-related CO_2 emissions (Suomie et al., 2025).

On a strength-normalized basis, the 50%RCA+20%RHA mixture exhibited the lowest GWP/f'c value (4.807 kg CO_2/MPa), outperforming the control (5.464 kg CO_2/MPa). Although the 100%RCA+20%RHA mixture had a lower overall GWP, its GWP/f'c value (5.657 kg CO_2/MPa) was less favorable due to the reduction in compressive strength. Therefore, moderate RCA replacement provided the best balance between carbon reduction and mechanical performance.

Acidification potential and AP-to-strength ratio

Figure 10(c) shows that the incorporation of RHA and RCA significantly reduced acidification potential (AP). The control mixture recorded

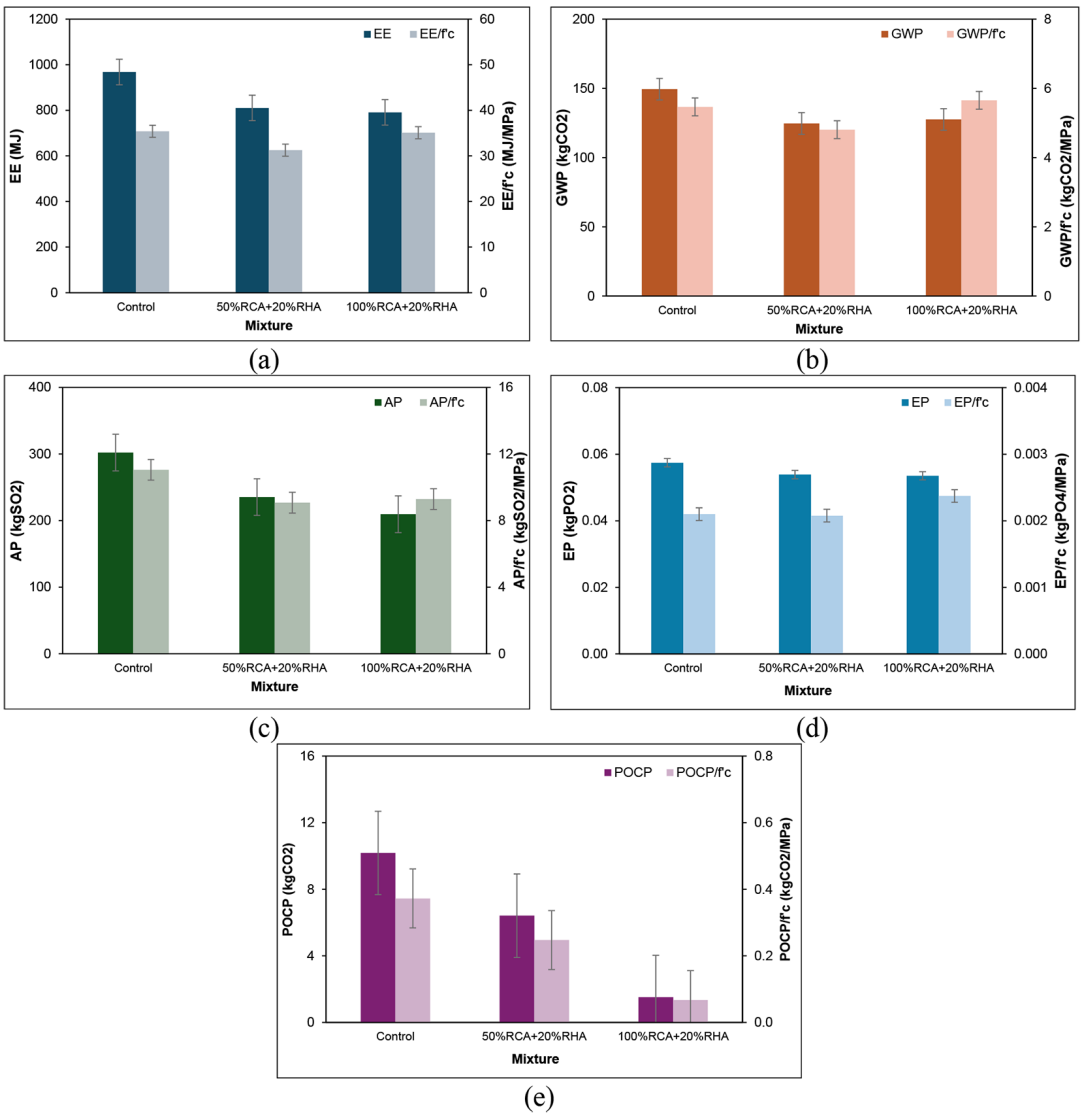

Figure 10. LCA results of concrete mixtures incorporating RCA and RHA with their corresponding impact-to-strength ratios: (a) EE, (b) GWP, (c) AP, (d) EP, and (e) POC

the highest AP (302.110 kg SO_2/m^3), while the 50%RCA+20%RHA and 100%RCA+20%RHA mixtures achieved values of 235.281 and 209.461 kg SO_2/m^3, corresponding to reductions of 22.1% and 30.7%, respectively. This improvement is mainly attributed to the reduced clinker content, which lowered emissions of sulfur oxides and other acidifying substances.

The AP/f'c results showed that the 50%RCA+20%RHA mixture had the lowest value (9.075 kg SO_2/MPa), compared with 11.046 kg SO_2/MPa for the control. Although the 100%RCA+20%RHA mixture achieved the lowest overall AP, its AP/f'c value slightly increased (9.289 kg SO_2/MPa) due to the reduction in compressive strength. Therefore, moderate RCA replacement provided the most favorable balance between acidification reduction and mechanical performance.

Eutrophication potential and EP-to-strength ratio

Figure 10(d) shows that the incorporation of RHA and RCA slightly reduced eutrophication potential (EP). The control mixture recorded an EP of 5.742×10^{-2} kg PO_4 eq/m^3, while the 50%RCA+20%RHA and 100%RCA+20%RHA mixtures achieved values of 5.387×10^{-2} and 5.351×10^{-2} kg PO_4 eq/m^3, respectively. Although the reductions were modest, they indicate lower nutrient-related emissions associated with the use of recycled materials.

For the EP/f'c ratio, the 50%RCA+20%RHA mixture exhibited the lowest value (2.078×10^{-3} kg PO_4 eq/MPa), comparable to the control

(2.100×10^{-3} kg PO_4 eq/MPa). In contrast, the 100%RCA+20%RHA mixture showed a higher EP/f'c value (2.373×10^{-3} kg PO_4 eq/MPa) due to its lower compressive strength. These results indicate that moderate RCA replacement provides a more favorable balance between eutrophication impact and mechanical performance.

Photochemical ozone creation potential and POCP-to-strength ratio

Figure 10(e) shows that the incorporation of RHA and RCA substantially reduced photochemical ozone creation potential (POCP). The control mixture exhibited the highest POCP (10.185 kg C_2H_4/m^3), while the 50%RCA+20%RHA and 100%RCA+20%RHA mixtures achieved values of 6.419 and 1.522 kg C_2H_4/m^3, corresponding to reductions of 37.0% and 85.1%, respectively. This improvement is attributed to the reduced consumption of virgin materials and lower emissions from cement and aggregate production.

A similar trend was observed for the POCP/f'c ratio, which decreased from 0.372 kg C_2H_4/MPa for the control to 0.248 and 0.067 kg C_2H_4/MPa for the 50%RCA+20%RHA and 100%RCA+20%RHA mixtures, respectively. Unlike the other strength-normalized indicators, POCP/f'c continued to improve with increasing RCA content, indicating that the reduction in POCP emissions outweighed the loss in compressive strength.

Interdependence of the energy and environmental impact-to-strength ratios

Based on the obtained results, the relationships among the environmental impact-to-strength ratios, including EE/f'c, GWP/f'c, AP/f'c, EP/f'c, and POCP/f'c, the values of which are presented in Figure 10. With only three mixtures, these values are presented as descriptive observations rather than as statistically estimated correlations.

Because only three mixtures were tested (n = 3), no correlation coefficients, p-values, or statistical-significance claims are reported, as such statistics are not meaningful at this sample size. The indicators are therefore compared descriptively. EE/f'c and GWP/f'c move together across the three mixtures, which is expected because both are governed primarily by Portland-cement (clinker) content; reducing clinker through RHA substitution lowers both simultaneously. POCP/f'c, by contrast, varies independently of the energy- and carbon-related indicators and is dominated by the large difference between the natural- and recycled-aggregate inventory factors used here (Table 4).

Multi criteria analysis of energy and environmental impact-to-strength ratios

MCDM analysis was conducted to evaluate the combined energy and environmental performance of the investigated concrete mixtures by integrating multiple impact-to-strength indicators into a unified framework. Five indicators were considered, namely EE/f'c, GWP/f'c, AP/f'c, EP/f'c, and POCP/f'c, which represent the environmental impacts associated with each unit of compressive strength. To enable direct comparison, all indicators were normalized to a common scale.

Figure 11 presents the radar chart of the normalized indicators of the mixtures. The radar chart serves only as a visual summary and was not used for formal ranking. Based on the enclosed areas, the Control mixture showed the lowest overall performance (1.261), followed by 50%RCA+20%RHA (1.686), while 100%RCA+20%RHA achieved the largest area (2.002), indicating the most balanced environmental impact-to-strength performance. This result is mainly attributed to its substantially lower POCP/f'c and relatively low EE/f'c and GWP/f'c values compared with the Control mixture.

To confirm that the ranking was not an artifact of the radar-area representation, the same indicators were re-evaluated using TOPSIS with equal weights as depicted in Table 8. The TOPSIS procedure involved normalization of the decision matrix, weighting of the normalized values, determination of the positive- and negative-ideal solutions, calculation of separation distances, and estimation of the relative closeness coefficient using Equations 10–14. Treating all indicators as cost criteria, the relative closeness coefficients were 0.098 for the Control, 0.451 for 50%RCA+20%RHA, and 0.832 for 100%RCA+20%RHA, producing the identical ranking: 100%RCA+20%RHA > 50%RCA+20%RHA > Control. However, indicator-level analysis showed that 50%RCA+20%RHA performed best for EE/f'c, GWP/f'c, AP/f'c, and EP/f'c, whereas only POCP/f'c favored full RCA replacement. Sensitivity analysis further revealed that POCP/f'c strongly influenced the final ranking. When POCP/f'c was excluded, the ranking changed to 50%RCA+20%RHA > 100%RCA+20%RHA

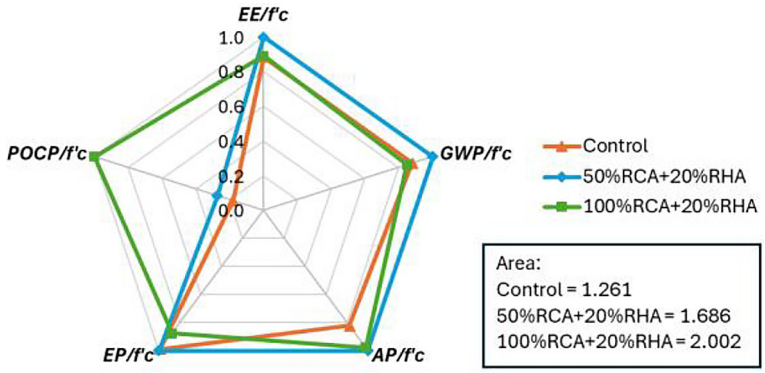

Figure 11. Multi criteria analysis

Table 8. Decision matrix of strength-normalised energy and environmental indicators

Mixture	EE/f'c (MJ/MPa)	GWP/f'c (kg CO_2/MPa)	AP/f'c (kg SO_2/MPa)	EP/f'c (kg PO_4/MPa)	POCP/f'c (kg C_2H_4/MPa)
Control	35.398	5.464	11.046	2.100×10^{-3}	0.372
50%RCA+20%RHA	31.265	4.807	9.075	2.078×10^{-3}	0.248
100%RCA+20%RHA	35.084	5.657	9.289	2.373×10^{-3}	0.067

> Control, indicating that the preference for full RCA replacement depends on the adopted weighting scheme and POCP inventory assumptions.

$$r_{ij} = x_{ij} / \sqrt{(\Sigma_i x_{ij}^2)} \quad (10)$$

$$v_{ij} = w_j \cdot r_{ij}, \Sigma_j w_j = 1 \quad (11)$$

$$A^+ = \{ min_i v_{ij} \}, A^- = \{ max_i v_{ij} \} \quad (12)$$

$$d_i^+ = \sqrt{[\Sigma_j (v_{ij} - v_j^+)^2]}, \quad d_i^- = \sqrt{[\Sigma_j (v_{ij} - v_j^-)^2]} \quad (13)$$

$$C_i = d_i^- / (d_i^+ + d_i^-) \quad (14)$$

where: x_{ij} is the value of criterion j for mixture i, w_j is the weight of criterion j, v_j^+ and v_j^- are the positive- and negative-ideal weighted values of criterion j, and a higher closeness coefficient C_i denotes a more favourable overall performance.

The resulting separation distances and closeness coefficients are summarised in Table 9. Under equal weighting the procedure yields C_i = 0.832, 0.451 and 0.098 for the 100%RCA+20%RHA, 50%RCA+20%RHA and Control mixtures, respectively, giving the ranking 100%RCA+20%RHA > 50%RCA+20%RHA > Control. These values reproduce the closeness coefficients reported above and confirm that the ranking obtained from the formal TOPSIS computation is consistent with the descriptive radar-chart visualisation.

The radar chart also demonstrates that the 50%RCA+20%RHA mixture exhibited relatively high normalized values for EE/f'c and GWP/f'c, which resulted in a larger environmental burden compared with the 100%RCA+20%RHA mixture. In contrast, the Control mixture showed the smallest polygonal area due to its comparatively poorer performance in several environmental indicators, particularly AP/f'c and EP/f'c. These findings indicate that the combined use of RHA and RCA can effectively enhance the environmental sustainability of concrete when evaluated simultaneously across multiple criteria rather than through a single environmental indicator alone.

Overall, the MCDM and TOPSIS analysis identifies the 100%RCA+20%RHA mixture as providing the most favorable aggregate balance between energy consumption, environmental impacts, and compressive strength performance under equal criterion weighting. This diagram outcome should be read together with the per-indicator results, which favour the 50%RCA+20%RHA mixture on four of the five ratios; the "best" mixture is therefore weighting-dependent rather than unique. Taken together, the analyses demonstrate that the incorporation of agricultural and construction waste materials has considerable potential to improve the sustainability performance of concrete mixtures.

Table 9. TOPSIS separation distances, closeness coefficients, and ranking of the concrete mixtures (equal weights, all cost criteria)

Mixture	d^+	d^-	C_i	Rank
Control	0.138	0.015	0.098	3
50%RCA+20%RHA	0.080	0.066	0.451	2
100%RCA+20%RHA	0.028	0.137	0.832	1

CONCLUSIONS

The objective of this study was successfully achieved through the integrated assessment of the mechanical behaviour and environmental performance of concrete RHA and RCA. The results demonstrated that the combined use of agricultural and construction-demolition waste materials can substantially reduce environmental burdens while maintaining acceptable engineering performance, although the extent of the benefit depends on the selected sustainability criteria.

The results revealed that the 50%RCA+20%RHA mixture provided the most balanced compromise between mechanical performance and environmental efficiency, achieving the lowest values for most strength-normalized environmental indicators. In contrast, the 100%RCA+20%RHA mixture achieved the lowest overall environmental burdens and was identified as the preferred alternative under equal-weight TOPSIS evaluation. However, the sensitivity analysis showed that this preference depends strongly on the weighting assumptions and the influence of the POCP indicator, highlighting the importance of transparent sustainability criteria in material-selection decisions.

The study contributes to the existing body of knowledge by providing a unified evaluation framework that combines experimental stress–strain characterization, constitutive modelling, life-cycle environmental assessment, and multi-criteria sustainability analysis for RHA–RCA concrete. Overall, the findings confirm the potential of combining agricultural and construction-demolition waste streams as a resource-recovery strategy for lower-impact concrete production.

This study evaluated only 28-day mechanical properties and cradle-to-gate environmental impacts. Durability performance, economic feasibility, and the variability of field-sourced RCA were not considered. In addition, only three mixtures were tested, limiting statistical inference and the robustness of the TOPSIS ranking. The post-peak stress–strain response was also defined by a limited number of data points. Future studies should incorporate durability testing, cost analysis, field-sourced RCA, and larger experimental datasets to validate the applicability of RHA–RCA concrete for structural applications.

REFERENCES

1. Ahmad, S., Upadhyay, S., Umar, A., Al-Osta, M. A. (2023). Effect of recycled crushed glass and recycled coarse aggregate on the properties of self-compacting concrete. *Case Studies in Construction Materials, 19*, e02532. https://doi.org/10.1016/j.cscm.2023.e02532
2. Ahmed, A., Hyndman, F., Kamau, J., Fitriani, H. (2020). Rice husk ash as a cement replacement in high strength sustainable concrete. *Materials Science Forum, 1007*, 90–98. https://doi.org/10.4028/www.scientific.net/MSF.1007.90
3. An, T., Li, J., Lin, Q., Li, G. (2024). Ozone formation potential related to the release of volatile organic compounds (VOCs) and nitrogen oxide (NOX) from a typical industrial park in the Pearl River Delta. *Environmental Science: Atmospheres, 4*(11), 1229–1238. https://doi.org/10.1039/D4EA00091A
4. ApS, V. V. (2025). Verified Environmental Product Declaration | ISO 14025 & EN 15804. In MD-25171-EN. EPD Danmark. https://www.epddanmark.dk/media/h4nntjsb/md-25171-en.pdf
5. ASTM C33/C33M. Standard Specification for Concrete Aggregates. ASTM International, West Conshohocken, PA.
6. ASTM C39/C39M. Standard Test Method for Compressive Strength of Cylindrical Concrete Specimens. ASTM International, West Conshohocken, PA.
7. ASTM C469/C469M. Standard Test Method for Static Modulus of Elasticity and Poisson's Ratio of Concrete in Compression. ASTM International, West Conshohocken, PA.
8. Bare, J. C., Norris, G. A., Pennington, D. W., McKone, T. (2002). TRACI. *Journal of Industrial Ecology, 6*(3–4), 49–78. https://doi.org/10.1162/108819802766269539

9. BPS-Statistics Indonesia. (2024). Harvested Area, Productivity, and Production of Paddy in Indonesia, 2023. *BPS-Statistics Indonesia, Jakarta.*
10. Cabeza, L. F., Rincón, L., Vilariño, V., Pérez, G., Castell, A. (2014). Life cycle assessment (LCA) and life cycle energy analysis (LCEA) of buildings and the building sector: A review. *Renewable and Sustainable Energy Reviews, 29*, 394–416. https://doi.org/10.1016/j.rser.2013.08.037
11. Carreira, D. J., Chu, K. H. (1985). Stress–strain relationship for plain concrete in compression. ACI Journal Proceedings, 82(6), 797–804.
12. Cherian, P., Palaniappan, S., Menon, D., Anumolu, M. P. (2020). Comparative study of embodied energy of affordable houses made using GFRG and conventional building technologies in India. *Energy and Buildings, 223*, 110138. https://doi.org/10.1016/j.enbuild.2020.110138
13. Dixit, M. K., Fernández-Solís, J. L., Lavy, S., Culp, C. H. (2010). Identification of parameters for embodied energy measurement: A literature review. *Energy and Buildings, 42*(8), 1238–1247. https://doi.org/10.1016/j.enbuild.2010.02.016
14. Eurostat. (2022). Waste statistics – Generation of waste by economic activity (construction and demolition waste). *Statistical Office of the European Union, Luxembourg*.
15. Fernando, S., Gunasekara, C., Law, D. W., Nasvi, M. C. M., Setunge, S., Dissanayake, R. (2021). Life cycle assessment and cost analysis of fly ash–rice husk ash blended alkali-activated concrete. *Journal of Environmental Management, 295*, 113140. https://doi.org/10.1016/j.jenvman.2021.113140
16. Flower, D. J. M., Sanjayan, J. G. (2007). Greenhouse gas emissions due to concrete manufacture. *The International Journal of Life Cycle Assessment, 12*(5), 282–288. https://doi.org/10.1065/lca2007.05.327
17. Government Regulation of the Republic of Indonesia No. 27 of 2020 (PP No. 27/2020) concerning Specific Waste Management (Pengelolaan Sampah Spesifik). Jakarta, Indonesia.
18. Guinée, J. B., Gorrée, M., Heijungs, R., et al. (2002). *Handbook on life cycle assessment: operational guide to the ISO Standards.* Kluwer Academic Publishers, Dordrecht.
19. Habert, G., D'Espinose De Lacaillerie, J. B., Roussel, N. (2011). An environmental evaluation of geopolymer based concrete production: Reviewing current research trends. *Journal of Cleaner Production, 19*(11), 1229–1238. https://doi.org/10.1016/j.jclepro.2011.03.012
20. Hammond, G., Jones, C., Lowrie, F., Tse, P. (2011). Embodied carbon: The Inventory of Carbon and Energy (ICE). *BSRIA.*
21. Huang, X., Huang, Z., Zhou, Y., Hu, R., Hu, B. (2025). Life cycle assessment and cost analysis of LC3 concrete considering sustainability and uncertainty. *Journal of Building Engineering, 102*, 111960. https://doi.org/10.1016/j.jobe.2025.111960
22. Hwang, C. L., Yoon, K. (1981). *Multiple Attribute Decision Making: Methods and Applications*. Lecture Notes in Economics and Mathematical Systems, Vol. 186. Springer-Verlag, Berlin. https://doi.org/10.1007/978-3-642-48318-9
23. Kim, T., Tae, S., Chae, C. U. (2016). Analysis of environmental impact for concrete using LCA by varying the recycling components, the compressive strength and the admixture material mixing. Sustainability, 8(4), 389. https://doi.org/10.3390/su8040389
24. Kina, C., Turk, K. (2025). Workability, flexural response and shrinkage crack restriction of fiber-reinforced SCC: Effects of low coarse aggregate content and micro fiber type. *Construction and Building Materials, 491*, 142586. https://doi.org/10.1016/j.conbuildmat.2025.142586
25. Liu, C., Zhang, W., Liu, H., Zhu, C., Wu, Y., He, C., Wang, Z. (2022). Recycled aggregate concrete with the incorporation of rice husk ash: Mechanical properties and microstructure. *Construction and Building Materials, 351*, 128934. https://doi.org/10.1016/j.conbuildmat.2022.128934
26. Ma, W., Lv, B., Wang, Y., Huang, L., Yan, L., Kasal, B. (2024). Freeze–thaw, chloride penetration and carbonation resistance of natural and recycled aggregate concrete containing rice husk ash as replacement of cement. *Journal of Building Engineering, 86*, 108889. https://doi.org/10.1016/j.jobe.2024.108889
27. Mohammad, A. A. S., Mohammad, S. I., Oraini, B. Al, Alenazi, S. A., Vasudevan, A., Hassanshahi, O. (2025). Assessing the eco-efficiency of high recycled content pavement solutions: An evaluation of the mechanical, durability, and environmental impacts. *Journal of Composites Science, 9*(12), 692. https://doi.org/10.3390/jcs9120692
28. Ohemeng, E. A., Naghizadeh, A. (2023). Alternative cleaner production of masonry mortar from fly ash and waste concrete powder. *Construction and Building Materials, 374*, 130859. https://doi.org/10.1016/j.conbuildmat.2023.130859
29. Park, W. J., Kim, T., Roh, S., Kim, R. (2019). Analysis of life cycle environmental impact of recycled aggregate. *Applied Sciences, 9*(5), 1021. https://doi.org/10.3390/app9051021
30. Patil, R. V. (2024). Recycling construction and demolition waste in the sector of construction. *Advances in Civil Engineering*, Article 6234010. https://doi.org/10.1155/2024/6234010
31. Plaza, P., Sáez del Bosque, I. F., Frías, M., Sánchez de Rojas, M. I., Medina, C. (2021). Use of recycled coarse and fine aggregates in structural eco-concretes: Physical and mechanical properties

and CO_2 emissions. *Construction and Building Materials, 285*, 122926. https://doi.org/10.1016/j.conbuildmat.2021.122926

32. Popovics, S. (1973). A numerical approach to the complete stress–strain curve of concrete. *Cement and Concrete Research, 3*(5), 583–599.
33. Rashid, K., Razzaq, A., Ahmad, M., Rashid, T., Tariq, S. (2020). Multi-criteria optimization of recycled aggregate concrete mixes. *Journal of Cleaner Production, 276*, 124316. https://doi.org/10.1016/j.jclepro.2020.124316
34. Ro, J. W., Cunningham, P. R., Miller, S. A., Kendall, A., Harvey, J. (2024). Technical, economic, and environmental feasibility of rice hull ash from electricity generation as a mineral additive to concrete. *Scientific Reports, 14*(1), 9158. https://doi.org/10.1038/s41598-024-59615-1
35. Saade, M. R. M., Yahia, A., Amor, B. (2020). How has LCA been applied to 3D printing? A systematic literature review and recommendations for future studies. *Journal of Cleaner Production, 244*, 118803. https://doi.org/10.1016/j.jclepro.2019.118803
36. Shah, M. C., Gupta, K. K., Nainwal, A., Negi, A., Kumar, V. (2021). Investigation of mechanical properties of concrete with natural aggregates partially replaced by recycled coarse aggregate (RCA). *Materials Today: Proceedings, 46*, 10315–10321. https://doi.org/10.1016/j.matpr.2020.12.456
37. Shi, X., Zhang, C., Liang, Y., Luo, J., Wang, X., Feng, Y., Li, Y., Wang, Q., Abomohra, A. E. F. (2021). Life cycle assessment and impact correlation analysis of fly ash geopolymer concrete. *Materials, 14*(23), 7375. https://doi.org/10.3390/ma14237375
38. Stocker, T. F., Qin, D., Plattner, G. K., Tignor, M. M. B., Allen, S. K., Boschung, J., Nauels, A., Xia, Y., Bex, V., Midgley, P. M. (2014). *Climate Change 2013: The Physical Science Basis.* Cambridge University Press. https://doi.org/10.1017/CBO9781107415324
39. Suomie, R. W., Mishra, B. P., Das, S. (2025). Performance of rice husk ash (RHA) and recycled coarse aggregate (RCA) for sustainable concrete: A review. *Next Materials, 8*, 100778. https://doi.org/10.1016/j.nxmate.2025.100778